Available online at www.sciencedirect.com
SCIENCE DIRECT®
Journal of Sound and Vibration 273 (2004) 295–316
JOURNAL OF SOUND AND VIBRATION
www.elsevier.com/locate/jsvi

Reducing errors in the identification of structural joint parameters using error functions

J.H. Wang*, S.C. Chuang

Sound and Vibration Laboratories, Department of Power Mechanical Engineering, National Tsing Hua University, Hsinchu, Taiwan

Received 11 October 2002; accepted 28 April 2003

Abstract

A new method is proposed to identify the structural joint parameters directly from the frequency response functions (FRFs) of the substructures and the whole structure. The problem of the measurement noise with non-Gaussian distribution in the FRFs, and the problem of joints with very different orders of magnitude are especially discussed in this work. The new method uses an error function to select the best data to identify the individual parameter so that the new method can function well under different strict conditions. The accuracy of the new method and other two existing methods is compared under different conditions in this work.

1. Introduction

In the past, computational simulation of structure dynamics has become more accurate, reliable and less expensive. However, the accuracy of dynamic simulation depends on the accuracy of the parameter of the structure. A real mechanical system usually consists of many components connected together through different joints (for example, sliding joint, bolted joint, etc.). The dynamic parameters of the joints generally are very difficult to know by theoretical methods. Therefore, great efforts have been made in the field of experimental parameters identification in the past. Some of the identification methods were developed to identify the parameters of the whole structure [1–7], some methods were specially developed for the identification of joint parameters [8–17]. Here only the methods to identify the joint parameters will be discussed.

*Corresponding author. Tel.: +886-3-5719034; fax: +886-3-5727873.
E-mail address: jhwang@mx.nthu.edu.tw (J.H. Wang).

0022-460X/03/$ - see front matter
doi:10.1016/S0022-460X(03)00502-9

Basically, there are two different approaches to identify the joint properties, one is the model-based approach; the other is the pure experimental approach. The model-based approach used both the experimental data and the theoretical model by the finite element methods (FEM) to identify the joint parameters [8–13]. The basic principle of the model-based approach is to minimize the error between the FEM model and the experimental data with different techniques or algorithms. The model-based approach has its advantages, for instance, many kinds of FEM software are available in the market, and FEM becomes a standard method for structure analysis. However, some modelling error may be introduced in the theoretical model by the finite element approximation, especially the damping property of the structure. One knows that the stiffness and mass properties of a structure generally can be accurately generated by the FEM, but the damping property of a structure (not include the joint to be identified) generally cannot be generated accurately by the FEM. The pure experimental approach uses only the experimental data to identify the joint parameters [14–17]. Although the pure experimental approach can use the experimental data in time domain or frequency domain to identify the joint parameters, the frequency response functions (FRFs) are widely used in this approach. The main advantage of the pure experimental approach is that the theoretical modelling error of the structure can be avoided. However, the most troublesome problem of this approach is the unavoidable noise in the measurement data. The method proposed by Tsai and Chou [14] directly used the measured FRFs of substructures and the whole structure to extract the joint parameters. The method [14] is very simple and can avoid the theoretical modelling error of the structure. However, the results showed that the method practically had serious problem due to the unavoidable noise in the measured FRFs. Because there are many advantages to use the FRFs directly to extract the joint parameters, two different methods [15,16] have been proposed to minimize the effect of noise in the measured FRFs. Although the methods [15,16] work well under normal conditions, and also have been applied successfully to identify the joint parameters of real machines [18,19], our long-term experiences show that the methods [15,16] may identify false results in some situations. The situations are:

(1) If the noise distribution is Gaussian or near Gaussian with zero mean value, the methods work well. However, if the noise distribution is non-Gaussian or Gaussian with mean value (DC bias), the identified results become worse.
(2) If the orders of magnitude of the joint parameters are different significantly, the joint parameters cannot be identified with reasonable accuracy, especially the smallest parameter.

In this work, a new identification algorithm is proposed to improve the identified results under the above conditions. Although the method proposed in this work also uses the measured FRFs to identify the joint parameters, and is the same as the previous works [15,16], for reference convenient, the theoretical formulation in the next section begins from the basic theory.

2. Theoretical formulation

A real mechanical system usually consists of many components connected together by different joints. Therefore, it is easy to divide the whole structure into substructures from the joints to be

identified. For simplicity, in the following formulation the whole structure is divided into two substructures from the joints to be identified, as shown in Fig. 1. It is assumed that the joints can be modelled as linear spring and damper elements, as indicated by k_i and d_i in Fig. 1. The objective of parameter identification is to extract the joint parameters from the frequency response functions (FRFs) of the whole structure and substructures. With the definition of FRFs, the relation between the displacement vectors and force vectors of substructures 1 and 2 (see Fig. 1) can be written as

$$\begin{Bmatrix} \{X_e\} \\ \{X_a\} \end{Bmatrix} = \begin{bmatrix} [H_{ee}]_1, [H_{ea}]_1 \\ [H_{ae}]_1, [H_{aa}]_1 \end{bmatrix} \begin{Bmatrix} \{F_e\}_1 \\ \{F_a\}_1 + \{F_j\}_1 \end{Bmatrix}, \tag{1}$$

$$\begin{Bmatrix} \{X_b\} \\ \{X_c\} \end{Bmatrix} = \begin{bmatrix} [H_{bb}]_2, [H_{bc}]_2 \\ [H_{cb}]_2, [H_{cc}]_2 \end{bmatrix} \begin{Bmatrix} \{F_b\}_2 + \{F_j\}_2 \\ \{F_c\}_2 \end{Bmatrix}, \tag{2}$$

where $\{X_a\}$ and $\{X_b\}$ represent the displacement vectors on the joint interfaces of substructures 1 and 2, respectively; $\{X_e\}$ and $\{X_c\}$ represent the displacement vectors on all other regions except the joint interfaces of substructures 1 and 2. The vectors $\{F_j\}_1$ and $\{F_j\}_2$ represent the joint internal force vectors acting on substructures 1 and 2. The vectors $\{F_a\}_1$ and $\{F_e\}_1$ represent the external force vectors acting on substructure 1, while the vectors $\{F_b\}_2$ and $\{F_c\}_2$ represent the external force vectors acting on substructure 2. The force vectors $\{F_j\}_1$ and $\{F_j\}_2$ are equal in magnitude and opposite in direction, i.e.,

$$\{F_j\}_1 = -\{F_j\}_2. \tag{3}$$

The interface displacement vectors $\{X_a\}$ and $\{X_b\}$ are related to the joint force vector by a transfer function $[H_j]$

$$\{X_b\} - \{X_a\} = [H_j]\{F_j\}_1 \tag{4}$$

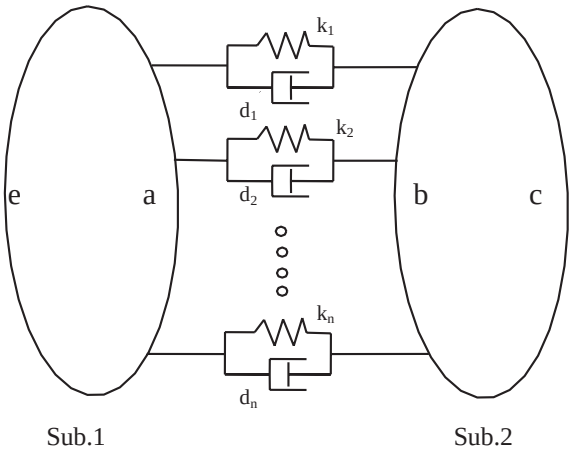

Fig. 1. A structure including two substructures connected by joints, $k_1, d_1, \ldots, k_n, d_n$.

with

$$[H_j] \equiv [P_j]^{-1} = \begin{bmatrix} k_1 + j\omega d_1 & 0, & 0, & \cdots & 0 \\ 0 & k_2 + j\omega d_2, & 0, & \cdots & 0 \\ 0 & \vdots & \ddots & & \vdots \\ \vdots & \vdots & & \ddots & \vdots \\ 0 & 0 & & & k_n + j\omega d_n \end{bmatrix}^{-1},$$

where $j = \sqrt{-1}$ and $k_1, k_2, \ldots, k_n, d_1, d_2, \ldots, d_n$ are the spring and damping coefficients of the joint.

If the whole structure is considered, the relation between the displacement vector and the force vector can be expressed as

$$\begin{Bmatrix} \{X_e\} \\ \{X_a\} \\ \{X_b\} \\ \{X_c\} \end{Bmatrix} = \begin{bmatrix} [H_{ee}], & [H_{ea}], & [H_{eb}], & [H_{ec}] \\ [H_{ae}], & [H_{aa}], & [H_{ab}], & [H_{ac}] \\ [H_{be}], & [H_{ba}], & [H_{bb}], & [H_{bc}] \\ [H_{ce}], & [H_{ca}], & [H_{cb}], & [H_{cc}] \end{bmatrix} \cdot \begin{Bmatrix} \{F_e\}_1 \\ \{F_a\}_1 \\ \{F_b\}_2 \\ \{F_c\}_2 \end{Bmatrix}. \tag{5}$$

As derived in the previous work [15], the FRFs of the whole structure in Eq. (5) can be expressed in terms of the FRFs of the substructures and the joint matrix $[H_j]$ in Eq. (4). For instance,

$$[H_{ee}] = [H_{ee}]_1 - [H_{ea}]_1[H_B]^{-1}[H_{ae}]_1, \tag{6a}$$

$$[H_{aa}] = [H_{aa}]_1 - [H_{aa}]_1[H_B]^{-1}[H_{aa}]_1, \tag{6b}$$

$$\begin{aligned} [H_{ba}] &= [H_{bb}]_2[H_B]^{-1}[H_{aa}]_1, \\ &\vdots \\ &\vdots \end{aligned} \tag{6c}$$

with

$$[H_B] = [H_{aa}]_1 + [H_{bb}]_2 + [H_j]. \tag{7}$$

Eq. (6) contains three different matrices, i.e., the FRFs of the substructures, the FRFs of the whole structure, and the joint matrix $[H_j]$. Therefore, if the FRFs of the substructures and the whole structure are known by experimental measurement, then the only unknowns in Eq. (6) are the joint parameters in $[H_j]$. Theoretically, the joint parameters can easily be obtained from Eq. (6) from the pure mathematical point of view. For instance, one can derive the unknown matrix $[H_j]^{-1} = [P_j]$ directly from Eq. (6b) as [14]

$$[P_j] = [H_{aa}]^{-1}[H_D][H_{aa}]^{-1} \tag{8}$$

with

$$[H_D] = (([H_{aa}]_1 - [H_{aa}])^{-1} - [H_{aa}]_1^{-1}([H_{aa}]_1 + [H_{bb}]_2)[H_{aa}]_1^{-1})^{-1}.$$

One can find that there are many inverse operations on the matrices in Eq. (8). Consequently, a little noise or measurement error in the FRFs will cause the identified results to be completely faulty because of the ill-conditioned problem. In other words, Eq. (8) is correct only from pure mathematical point of view, it cannot be applied to practical identification. To overcome the

problem found in Eq. (8), a method with the main objective to minimize the number of inverse operations has been proposed by Wang and Liou [15]. However, as mentioned, the previous methods [15,16] do not work well under some conditions.

The basic idea of the new method proposed in this work is based on the understanding about the limitations of the previous methods [15,16] according to our long-term experiences. From Eq. (A.5) in Appendix A, the $[P_j]$ matrix can be solved directly as

$$[P_j] = -([H_{aa}]_1 + [H_{bb}]_2)^{-1}([H_{aa}]_1 + [H_{ba}] - [H_{aa}])([H_{ba}] - [H_{aa}])^{-1}. \tag{9}$$

From Eq. (4) one knows that if all the FRF matrices in Eq. (9) are exact without any error, the $[P_j]$ matrix solved from Eq. (9) should be a diagonal matrix. On the contrary, if the FRF matrices in Eq. (9) are contaminated by noise, the $[P_j]$ matrix solved from Eq. (24) should not be a diagonal matrix. The new method proposed in this work is also based on Eq. (A.5), however, does not force the $[P_j]$ matrix to be a diagonal matrix. To distinguish from the theoretical $[P_j]$ defined in Eq. (4), a new matrix $[P_j^*]$ is defined as

$$\begin{aligned}[P_j^*] &\equiv \begin{bmatrix} p_1, & 0, & \cdots & \cdots & 0 \\ 0, & p_2 & \cdots & \cdots & 0 \\ \vdots & 0 & \ddots & & \vdots \\ \vdots & \vdots & & \ddots & \vdots \\ 0 & \cdots & \cdots & \cdots & p_n \end{bmatrix}_{n\times n} + \begin{bmatrix} \delta_{11}, & \delta_{12}, & \cdots & \cdots & \delta_{1n} \\ \delta_{21}, & \delta_{22}, & \cdots & \cdots & \delta_{2n} \\ \vdots & & & & \\ \vdots & & & & \\ \delta_{n1}, & \delta_{n2}, & \cdots & \cdots & \delta_{nn} \end{bmatrix}_{n\times n} \\ &= [P_j]_{n\times n} + [E]_{n\times n}, \end{aligned} \tag{10}$$

where

$$p_i = k_i + \mathrm{j}\omega d_i, \quad i = 1, 2, \ldots, n.$$

Now, the $[P_j]$ represents the matrix with the exact joint parameters and the $[E]$ matrix represents the error matrix. If the FRF matrices in Eq. (A.5) are contaminated by noise, then the $[P_j]$ matrix should be replaced by $[P_j^*]$. Then, Eq. (A.5) can be expanded as

$$\begin{bmatrix} u_{11}, & u_{12}, & \cdots & \cdots & u_{1n} \\ u_{21}, & u_{22}, & \cdots & \cdots & u_{2n} \\ \vdots & & & & \\ \vdots & & & & \\ u_{n1}, & u_{n2}, & \cdots & \cdots & u_{nn} \end{bmatrix} = \begin{bmatrix} s_{11}, & s_{12}, & \cdots & \cdots & s_{1n} \\ s_{21}, & s_{22}, & \cdots & \cdots & s_{2n} \\ \vdots & & & & \\ \vdots & & & & \\ s_{n1}, & s_{n2}, & \cdots & \cdots & s_{nn} \end{bmatrix} \begin{bmatrix} p_1^*, & \delta_{12}, & \cdots & \cdots & \delta_{1n} \\ \delta_{21}, & p_2^*, & \cdots & \cdots & \delta_{2n} \\ \vdots & & & & \\ \vdots & & & & \\ \delta_{n1}, & \delta_{n2}, & \cdots & \cdots & p_n^* \end{bmatrix} \begin{bmatrix} t_{11}, & t_{12}, & \cdots & \cdots & t_{1n} \\ t_{21}, & t_{22}, & \cdots & \cdots & t_{2n} \\ \vdots & & & & \\ \vdots & & & & \\ t_{n1}, & t_{n2}, & \cdots & \cdots & t_{nn} \end{bmatrix}, \tag{11}$$

where $p_i^* = p_i + \delta_{ii}$

or

$$\begin{bmatrix} \begin{bmatrix} s_{11}t_{11} & \cdots & s_{11}t_{n1} \\ s_{11}t_{12} & \cdots & s_{11}t_{n2} \\ \vdots & \ddots & \vdots \\ s_{11}t_{1n} & \cdots & s_{11}t_{nn} \end{bmatrix} & \begin{bmatrix} s_{12}t_{11} & \cdots & s_{12}t_{n1} \\ s_{12}t_{12} & \cdots & s_{12}t_{n2} \\ \vdots & \ddots & \vdots \\ s_{12}t_{1n} & \cdots & s_{12}t_{nn} \end{bmatrix} & \cdots & \cdots & \begin{bmatrix} s_{1n}t_{11} & \cdots & s_{1n}t_{n1} \\ s_{1n}t_{12} & \cdots & s_{1n}t_{n2} \\ \vdots & \ddots & \vdots \\ s_{1n}t_{1n} & \cdots & s_{1n}t_{nn} \end{bmatrix} \\ \vdots & & & & \vdots \\ \begin{bmatrix} s_{n1}t_{11} & \cdots & s_{n1}t_{n1} \\ s_{n1}t_{12} & \cdots & s_{n1}t_{n2} \\ \vdots & \ddots & \vdots \\ s_{n1}t_{1n} & \cdots & s_{n1}t_{nn} \end{bmatrix} & \begin{bmatrix} s_{n2}t_{11} & \cdots & s_{n2}t_{n1} \\ s_{n2}t_{12} & \cdots & s_{n2}t_{n2} \\ \vdots & \ddots & \vdots \\ s_{n2}t_{1n} & \cdots & s_{n2}t_{nn} \end{bmatrix} & \cdots & \cdots & \begin{bmatrix} s_{nn}t_{11} & \cdots & s_{nn}t_{n1} \\ s_{nn}t_{12} & \cdots & s_{nn}t_{n2} \\ \vdots & \ddots & \vdots \\ s_{nn}t_{1n} & \cdots & s_{nn}t_{nn} \end{bmatrix} \end{bmatrix}_{n^2\times n^2}$$

$$\times \begin{Bmatrix} \begin{Bmatrix} p_1^* \\ \delta_{12} \\ \vdots \\ \delta_{1n} \end{Bmatrix} \\ \begin{Bmatrix} \delta_{21} \\ p_2^* \\ \vdots \\ \delta_{2n} \end{Bmatrix} \\ \vdots \\ \begin{Bmatrix} \delta_{n1} \\ \vdots \\ \delta_{n(n-1)} \\ p_n^* \end{Bmatrix} \end{Bmatrix}_{n^2\times 1} = \begin{Bmatrix} \begin{Bmatrix} u_{11} \\ u_{12} \\ \vdots \\ u_{1n} \end{Bmatrix} \\ \begin{Bmatrix} u_{21} \\ u_{22} \\ \vdots \\ u_{2n} \end{Bmatrix} \\ \vdots \\ \begin{Bmatrix} u_{n1} \\ u_{n2} \\ \vdots \\ u_{nn} \end{Bmatrix} \end{Bmatrix}_{n^2\times 1} \tag{12}$$

or in a compact form

$$[A(\omega)]_{n^2\times n^2}\{P_r^*\}_{n^2\times 1} = \{B(\omega)\}_{n^2\times 1}. \tag{13}$$

Noting that the $[A]$ matrix and $\{B\}$ vector contain the information of FRFs, and are function of frequency ω. The $\{P_r^*\}$ vector contains the joint parameters p_i and the errors δ_{ij} defined in Eq. (10). If the joint parameters are frequency independent, then theoretically one only needs the data of the FRFs at one frequency to obtain the joint parameters by

$$\{P_r^*\}_{n^2\times 1} = [A(\omega)]^{-1}_{n^2\times n^2}\{B(\omega)\}_{n^2\times 1}. \tag{14}$$

However, due to the unavoidable measurement noise in the FRFs, like many existing methods, the FRFs at many discrete frequencies should be used to minimize the noise effect by using different algorithms. The new method proposed in this work uses the errors δ_{ij} $(i \neq j)$ as an indicator to find the best frequencies for identification. The details are derived in what follows.

The $[A]$ matrix and $\{B\}$ vector in Eq. (13) contain the information of FRFs. If the FRFs are exact (free from any error or noise), the $[A]$ matrix is indicated as $[A_0]$ and $\{B\}$ vector is indicated as $\{B_0\}$. Theoretically, if the $[A_0]$ and $\{B_0\}$ are exact, one can obtain the exact joint parameters from Eq. (13) because there is no approximation in deriving Eq. (13). Then Eq. (13) can be written as

$$[A_0(\omega)]_{n^2 \times n^2} \{P_{r0}\}_{n^2 \times 1} = \{B_0(\omega)\} \tag{15}$$

with

$$\{P_{r0}\} = \left\{ \begin{array}{c} \left\{ \begin{array}{c} p_1 \\ 0 \\ \vdots \\ 0 \end{array} \right\} \\ \left\{ \begin{array}{c} 0 \\ p_2 \\ \vdots \\ 0 \end{array} \right\} \\ \vdots \\ \left\{ \begin{array}{c} 0 \\ \vdots \\ \vdots \\ p_n \end{array} \right\} \end{array} \right\}.$$

Noting that the p_i in the $\{P_{r0}\}$ vector represents the exact joint parameter, as defined in Eq. (10). Except the exact parameters p_i, all the other elements δ_{ij} in $\{P_{r0}\}$ are equal to zero. If the FRFs are contaminated by noise, then Eq. (13) can be written as

$$([A_0] + [\delta_A])(\{P_{r0}\} + \{\delta_p\}) = \{B_0\} + \{\delta_B\}. \tag{16}$$

The $[\delta_A]$ matrix and $\{\delta_B\}$ vector represent the noise components in $[A]$ and $\{B\}$, respectively. The vector $\{\delta_p\}$ represents the error vector of $\{P_r^*\}$. It can be proved [20] that if $\{P_r^*\}$ is solved by Eq. (14), then

$$\frac{\|\{\delta_p\}\|}{\|\{P_{r0}\}\|} \leqslant \frac{K(A_0)}{1 - (K(A_0)\|\{\delta_A\}\|/\|[A_0]\|)} \left(\frac{\|\{\delta_B\}\|}{\|\{B_0\}\|} + \frac{\|[\delta_A]\|}{\|[A_0]\|} \right), \tag{17}$$

where $\|\,\|$ denotes the 2-norm of matrix or vector and $K(A_0) = \|[A_0]\|\,\|[A_0]^{-1}\|$, defined as the condition number of $[A_0]$. Eq. (17) shows the upper bound of the error of the parameters relative to the exact values in terms of the relative errors of $[A]$ and $\{B\}$ and the condition number of $[A_0]$. Because $[A]$ and $\{B\}$ are function of frequency ω, the error vector $\{\delta_p\}$ is also function of ω. From

Eq. (17), one knows that if one wants to obtain an accurate result from Eq. (14), one should select the frequencies at which the condition number of $[A_0]$ and the relative errors of $[A]$ and $\{B\}$ are the smaller the better. Because one does not know the exact values of $[A]$ and $\{B\}$, it is impossible to know the frequencies at which the errors $\{\delta_B\}$ and $[\delta_A]$ are small. However, from Eqs. (12) and (16) one has

$$\|\{\delta_p\}\| = \left(\sum_{j=1}^{n}\sum_{i=1}^{n}\delta_{ij}^2\right)^{1/2}. \tag{18}$$

Because the upper bound of $\|\{\delta_p\}\|$ is constrained by the relation of Eq. (17), the individual value of δ_{ij} cannot be arbitrary. In other words, the δ_{ij} must have some relationships among each other. This is the basic finding of the proposed new method. As defined in Eqs. (10) and (12), the δ_{ii} represents the identified error of parameter p_i and δ_{ij} $(i \neq j)$ represents the other error. Now, two error functions are defined as

$$R_e(E_i) \equiv \left[\sum_{j=1}^{n}(R_e(\delta_{ij}))^2\right]^{1/2} \quad \text{for } i \neq j,$$

$$I_m(E_i) \equiv \left[\sum_{j=1}^{n}(I_m(\delta_{ij}))^2\right]^{1/2} \quad \text{for } i \neq j, \tag{19}$$

where "R_e" and "I_m" indicate the real part and imaginary part, respectively. Both the $R_e(E_i)$ and $I_m(E_i)$ are function of frequency. One knows that if the FRFs are exact, then $R_e(E_i)$, $I_m(E_i)$, $R_e(\delta_{ii})$ and $I_m(\delta_{ii})$ from Eq. (14) all should be equal to zero. If the FRFs are contaminated by noise, then $R_e(E_i)$, $I_m(E_i)$, $R_e(\delta_{ii})$ and $I_m(\delta_{ii})$ must have some values; however, the $R_e(E_i)$ plus $|R_e(\delta_{ii})|$ has upper bound, the same for $I_m(E_i)$ plus $|I_m(\delta_{ii})|$. Therefore, there must be a relationship between $R_e(E_i)$ and $|R_e(\delta_{ii})|$, the same for $I_m(E_i)$ and $|I_m(\delta_{ii})|$. Because the error in the FRFs generally is random noise, the $R_e(E_i)$ and $|R_e(\delta_{ii})|$ should only have a statistical relationship, not a deterministic relationship. A typical example is given in Appendix B to show what the statistical relationship means.

Because the errors $|R_e(\delta_{ii})|$ and $|I_m(\delta_{ii})|$ are statistically highly correlated with $R_e(E_i)$ and $I_m(E_i)$, respectively, one can select the frequencies with which the error $R_e(E_i)$ is relatively small to identify the parameter k_i and select other frequencies with which the error $I_m(E_i)$ is relatively small to identify the parameter d_i. To explain this concept clearly, a structure with two joint parameters are used here as an example. Eq. (14) can now be written as

$$\begin{Bmatrix} p_1+\delta_{11} \\ \delta_{12} \\ \delta_{21} \\ p_2+\delta_{22} \end{Bmatrix} = \begin{Bmatrix} p_1^* \\ \delta_{12} \\ \delta_{21} \\ p_2^* \end{Bmatrix} = \begin{bmatrix} s_{11}t_{11}, s_{11}t_{21}, s_{12}t_{11}, s_{12}t_{21} \\ s_{11}t_{12}, s_{11}t_{22}, s_{12}t_{12}, s_{12}t_{22} \\ s_{21}t_{11}, s_{21}t_{21}, s_{22}t_{11}, s_{22}t_{21} \\ s_{21}t_{12}, s_{21}t_{22}, s_{22}t_{12}, s_{22}t_{22} \end{bmatrix}^{-1} \begin{Bmatrix} u_{11} \\ u_{12} \\ u_{21} \\ u_{22} \end{Bmatrix}. \tag{20}$$

Noting that p_1 and p_2 represent the exact joint parameters, as defined in Eq. (10). As mentioned, if the necessary FRFs are known at some frequencies (for instance by measurement), for each discrete frequency one can use Eq. (20) to obtain the joint parameters. However, due to the errors in the FRFs are different at each frequency, and the condition number of the inverse matrix in Eq. (20) is also different for each frequency, the identified parameters from each frequency are

different. So, one can use the error $R_e(E_i)$ and $I_m(E_i)$ to select the "good" frequencies for identification. In this example $R_e(E_1) = |R_e(\delta_{12})|$, $R_e(E_2) = |R_e(\delta_{21})|$, $I_m(E_1) = |I_m(\delta_{12})|$ and $I_m(E_2) = |I_m(\delta_{21})|$, all are function of frequencies. In other words, the errors $R_e(E_i)$ and $I_m(E_i)$ are used as indicators to find the "good" data for identification. As to the question how many frequencies should be used for identification is discussed in Appendix B.

In summary, the basic identification equation of the proposed method is Eq. (14) with the selected FRFs data according to the errors $R_e(E_i)$ and $I_m(E_i)$. The average values of the parameters identified from all the selected frequencies are defined as the identified values. From Eq. (14), the average values are defined as

$$\{P_r, ave\}_{n^2\times 1} = \frac{1}{N_1}\left(\sum_{j=1}^{N_1} ([A(\omega_j)]^{-1}\{B(\omega_j)\})\right). \tag{21}$$

Here ω_j indicates the selected frequencies, and N_1 is the total number of frequencies used for identification.

3. Simulation results and discussions

As mentioned, the main objective of the proposed new method is to improve the accuracy of the previous methods [15,16] at some special conditions. Therefore, the following simulations are focused on these problems.

3.1. Definition of noise level

One knows that the most important step to obtain an accurate identification result is to measure the FRFs correctly by considering the different equipments and procedure used [21]. However, the measurement noise is always unavoidable. In principle, the best way to simulate the noise contaminated FRFs is to add noise to the measurement input and output in time domain, and then use the discrete Fourier transform to calculate the FRFs. However, the characteristics of the noise generally are specified in frequency domain, for instance, the concept of narrow band noise, white noise, etc. So, most of the works which use the FRFs to identify the parameters add proper noise distribution directly in frequency domain to the FRFs.

The definition of noise level is the same as that defined in Ref. [15]. However, the random noise used in Ref. [15] was Gaussian distribution with zero mean, the noise used in this work was Gaussian distribution with certain mean value. As well known, the Gaussian distribution is determined by two parameters, i.e., the mean value $\bar{m}$ and the standard deviation σ. If the $H_{ij}(\omega)$ represents the FRF between the ith and jth degrees of freedom of the structure, then the noise level γ is defined as [15]

$$\gamma^2 = \sigma^2/|H_{ij}(\omega)|^2_{max}, \tag{22}$$

where $|H_{ij}(\omega)|_{max}$ is the maximum absolute value of $H_{ij}(\omega)$ in the frequency range of interest. Therefore, if a mean value $\bar{m}$ and noise level γ are given, a set of random number with Gaussian distribution can be generated by a computer program. Noting that the FRFs are complex; two sets of random noise were added to the real and imaginary parts of the FRF, respectively. In the

following simulations, different mean values and different noise levels will be used to show the difference between the new method and the previous methods.

3.2. Simulated structure

The simulated structure consists of two parallel beams connected together through three linear joints, as shown in Fig. 2. The whole system was approximated by 14 finite beam elements. It was assumed that the beams possessed structural damping proportional to the mass and stiffness matrices. It was assumed that the joints parameters, k_1, k_2, k_3, d_1, d_2 and d_3 should be identified. Therefore, the whole structure was divided into two substructures from these joints. In order to simulate the FRFs obtained from experimental measurement, the maximum frequency of interest and the frequency resolution of the FRF spectrum were set to be 2000 and 5 Hz, respectively. In other words, there are 400 discrete frequencies in each FRF spectrum.

3.3. Simulation results and discussions

In the following simulations, three different noise distributions and two sets of joint parameters will be used, as shown in Tables 1 and 2. One can find that the stiffness parameters in the first set are same order of magnitude while the stiffness parameters in the second set are different in order of magnitude. As mentioned, there are 400 discrete frequencies in each FRF spectrum, then m in Eq. (A.11) is then equal to 400. The number N in Eq. (A.12) is then equal to 200. As to the proposed new method, forty frequencies (i.e., $N_1 = 40$ in Eq. (21)) are selected from the 400 frequencies by using the $R_e(E_i)$ and $I_m(E_i)$ as indicators, see the details in Appendix B.

Case 1: In this example, the noise distribution is D1 and the joint parameters are set 1 (S1). The results identified from Eq. (A.11), Eqs. (A.12) and (21) are shown in Table 3. Although the error from method [15] is somewhat larger, especially the error of damping, the identified results from all the three methods are accurate enough for engineering application. The results also demonstrate again that if the noise distribution is Gaussian with zero mean and the order of magnitude of the parameters is the same, then the previous methods [15,16] are accurate enough for practical application. The results of Table 3 will be used as a base for comparison with other cases in what follows.

Case 2. In this case, the noise distribution is D2 and the joint parameters are set 1 (S1). The difference between this case and case 1 is the noise distribution with mean value in this case. The mean value of a random noise is to simulate a constant measurement error (or called DC bias) for all the frequencies. For instance, if the measurement system is not correctly calibrated, then the measured FRFs may be contaminated by certain constant error for all the frequencies.

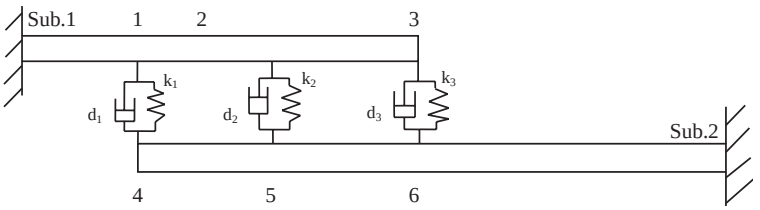

Fig. 2. Simulated structure.

Table 1
Three different noise distributions

Distributions	Noise parameters	
	Noise level v (%)	Mean value $\bar{m}$ (%)
D1 (Gaussian)	5	0
D2 (Gaussian with DC Bias)	5	0.1 of $\|H_{ij}(\omega)\|_{max}$
D3 (Non-Gaussian)	5 Multiplied by a frequency-dependent function	

Table 2
Two sets of joint parameters of the simulated structure

Parameters	Set 1	Set 2
k_1 (N/m)	1,000,000	10,000,000
k_2 (N/m)	2,000,000	200,000
k_3 (N/m)	1,500,000	50,000,000
d_1 (N s/m)	100	1000
d_2 (N s/m)	200	200
d_3 (N s/m)	150	1500

Table 3
Identified results of case 1

Parameters	Exact value	Identified value by Eq. (A.11) (error%)	Identified value by Eq. (A.12) (error%)	Identified value by Eq. (21) (error%)
k_1 (N/m)	1,000,000	1038024 (3.8%)	1021356 (2.13%)	986740 (1.32%)
k_2 (N/m)	2,000,000	2120314 (6.01%)	2010573 (0.52%)	2005681 (0.28%)
k_3 (N/m)	1,500,000	1561209 (4.08%)	1541829 (2.78%)	1486695 (0.88%)
d_1 (N s/m)	100	92 (8.00%)	103 (3.00%)	103 (3.00%)
d_2 (N s/m)	200	172 (14.00%)	195 (2.50%)	206 (3.00%)
d_3 (N s/m)	150	137 (8.67%)	146 (2.67%)	153 (2.00%)

To show the effect of noise on the FRFs, a typical FRF is shown in Figs. 3 and 4. Fig. 3 is the exact FRF of point 3 (see Fig. 2) of the whole structure, while Fig. 4 is the FRF contaminated by the noise. Because the constant error is only about 0.1% of the maximum value of the FRF, it is difficult to find out in the figure. However, the 5% random noise can easily be seen in Fig. 4. The

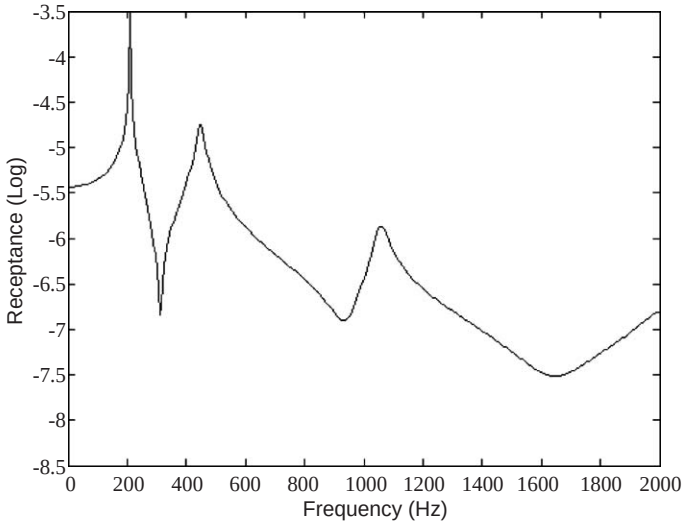

Fig. 3. A typical FRF without error.

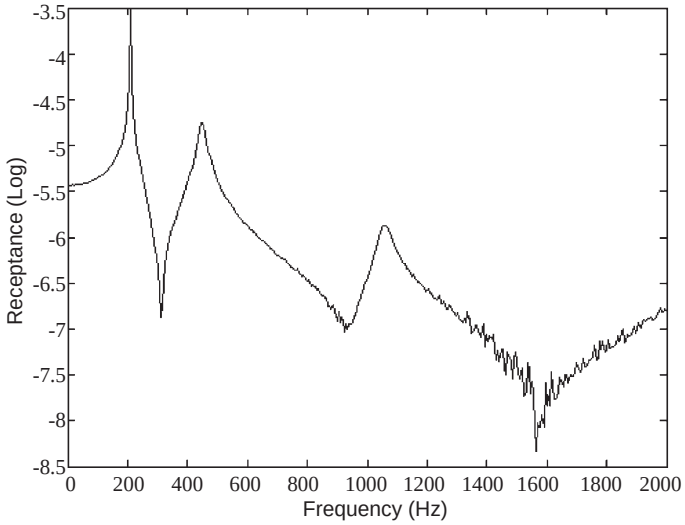

Fig. 4. The FRF in Fig. 3 contaminated by noise.

results identified by the three methods are listed in Table 4. The result identified by Eq. (A.11) [15] has significant error in comparison with other two methods. This is due to the fact that the least-squares method cannot effectively smooth the random noise with certain mean value. Although the method [16] (i.e., Eq. (A.12)) also cannot effectively smooth the random noise with certain DC bias, the method takes the condition number of the inverse matrix into consideration, and as a result, the error cause by ill-condition of the matrix can be reduced. That is why the result identified by Eq. (A.12) is better than that by Eq. (A.11). The results of Table 4 also demonstrate that the proposed new method can extract the joint parameters with best quality from the FRFs contaminated by random noise and DC bias.

Table 4
Identified results of case 2

Parameters	Exact value	Identified value by Eq. (A.11) (error%)	Identified value by Eq. (A.12) (error%)	Identified value by Eq. (21) (error%)
k_1 (N/m)	1,000,000	1114174 (11.41%)	1051533 (5.15%)	975662 (2.43%)
k_2 (N/m)	2,000,000	1740436 (12.97%)	2127693 (6.38%)	1901837 (4.90%)
k_3 (N/m)	1,500,000	1639910 (9.32%)	1408662 (6.08%)	1557789 (3.85%)
d_1 (N s/m)	100	78 (22.00%)	104 (4.00%)	97 (3.00%)
d_2 (N s/m)	200	228 (14.00%)	216 (8.00%)	185 (7.50%)
d_3 (N s/m)	150	119 (20.67%)	140 (6.67%)	155 (3.33%)

Case 3: In this case, the noise distribution is D3 and the joint parameters are set 1 (S1). The noise distribution is no more a Gaussian distribution. The noise distribution was generated by the following two steps:

(1) Giving the noise level 5% and using Eq. (22) to find the standard deviation σ. With the standard deviation σ, and mean value $\bar{m} = 0$, a set of random noise with Gaussian distribution was generated.
(2) The noise with Gaussian distribution was then multiplied by a frequency-dependent function.

Fig. 5 shows an example of the noise generated by the above procedure. The noise level is not uniformly distributed along the frequency axis, i.e., the noise level is larger at high frequency than at low frequency. It is easy to generate different types of random noise with non-Gaussian distribution. The noise distribution used in this case is just an arbitrary type. The identified results are listed in Table 5. One can find that the results identified by the previous methods [15,16] are unacceptable. Although the method [16] has taken the condition number of the $[Q]$ matrix into consideration, the order of error is the same as another method [15]. The reason for it can be explained as follows. As shown in Eq. (17), the upper bound of the error identified by Eq. (A.12) depends on the condition number of $[Q]$ and the relative measurement errors (noise) in $[Q]$ and $\{U\}$. Because the method [16] only uses the condition number of $[Q]$ to select frequencies for identification, it can happen that the measurement noise in $[Q]$ and $\{U\}$ is very large at the selected frequencies. From the result of Eq. (17) one knows that both the condition number and the noise in the FRFs should be considered in order to obtain an accurate result. However, so far no method can know the noise level at each frequency of the FRFs. Consequently, it is impossible to select the frequencies with less measurement noise for identification. The new method proposed in this work uses the $R_e(E_i)$ and $I_m(E_i)$ as indicators to select the frequencies (40 frequencies from 400 frequencies) at which the right hand side of Eq. (17) has smallest value among all the frequencies. That is why the result identified by the proposed new method is very accurate.

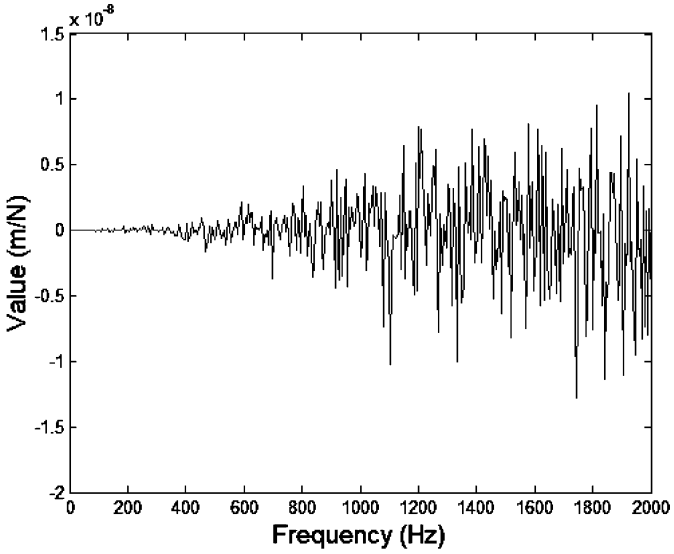

Fig. 5. The noise with non-Gaussian distribution.

Table 5
Identified results of case 3

Parameters	Exact value	Identified value by Eq. (A.11) (error%)	Identified value by Eq. (A.12) (error%)	Identified value by Eq. (21) (error%)
k_1 (N/m)	1,000,000	1399894 (39.98%)	1442905 (44.29%)	1009216 (0.92%)
k_2 (N/m)	2,000,000	3008194 (50.40%)	2874634 (43.73%)	2062468 (3.12%)
k_3 (N/m)	1,500,000	2110821 (40.72%)	2292620 (52.84%)	1533882 (2.25%)
d_1 (N s/m)	100	172 (72.00%)	202 (102.00%)	104 (4.00%)
d_2 (N s/m)	200	436 (118.00%)	380 (90.00%)	215 (7.50%)
d_3 (N s/m)	150	245 (63.33%)	279 (86.00%)	152 (1.33%)

The results of Tables 3–5 demonstrate that the proposed new method is superior to the previous methods. Of cause, the identified results of the new method will also become worse with higher noise level.

Case 4: The noise distribution is the same as case 2 (i.e., D2); however, the joint parameters are set 2 (S2). This example is used to show the difficulty when the orders of magnitude of the parameters are different significantly. The identified results are shown in Table 6. One finds that the results identified by the previous methods are unacceptable. In comparison with the results of Table 4, there are two factors which make the results of Tables 4 and 6 so different. The first factor is that the stiffness of k_1 and k_3 in this case becomes stiffer so that the relative defection at

Table 6
Identified results of case 4

Parameters	Exact value	Identified value by Eq. (A.11) (error%)	Identified value by Eq. (A.12) (error%)	Identified value by Eq. (21) (error%)
k_1 (N/m)	10,000,000	2299513 (77.0%)	11497137 (14.97%)	9554416 (4.45%)
k_2 (N/m)	200,000	8629417 (4214.70%)	5662639 (2731.31%)	188126 (5.93%)
k_3 (N/m)	50,000,000	38416040 (23.16%)	25028426 (49.94%)	51892310 (3.78%)
d_1 (N s/m)	1000	200 (80.00%)	1764 (76.40%)	1043 (4.30%)
d_2 (N s/m)	200	3726 (1764.50%)	671 (235.50%)	217 (8.50%)
d_3 (N s/m)	1500	6392 (326.13%)	2145 (43.00%)	1453 (3.13%)

the joint interfaces becomes smaller in the frequency range of simulation 0–2 kHz. Physically, if the joint stiffness becomes stiffer, the variation of the joint parameters has less effect on the variation of the FRFs, or, the sensitivity of the joint parameters to the FRFs becomes smaller in the frequency range 0–2 kHz. Consequently, the parameters are more difficult to identify from the FRF data. The second factor is that Eq. (A.11) (the same for Eq. (A.12)) uses the same data to identify all the parameters k_i and d_i. Theoretically, one should use different data (the most sensitive data) to identify different parameters, especially when the orders of magnitude of the parameters are different. The only question is how one can find different sets of data for the identification of different parameters. The new method proposed in this work uses $R_e(E_i)$ to select the best data to identify k_i, and uses $I_m(E_i)$ to select the best data to identify d_i. There are six parameters, i.e., k_1, k_2, k_3, d_1, d_2 and d_3, to be identified, six different sets of data are used in the new method. This is the reason why the new method is superior to other two methods.

Case 5: In this case, the noise distribution is non-Gaussian distribution (D3) and the joint parameters are set 2. This example is to simulate the worst conditions which may be encountered in practical application. The identified results are listed in Table 7. One can see that the results identified by Eqs. (A.11) and (A.12) are very poor, especially the smallest parameters, i.e., k_2 and d_2. These results are expected because the conditions used in this case are designed to expose the two main situations which may make the previous methods to collapse. The results of Table 7 also demonstrate that the proposed new method can overcome the limitations of previous methods, and result in an accurate result under serious conditions. It should be emphasized that one can generate many different types of noise with non-Gaussian distribution. As far as we have tested, the proposed new method always can identify a better result than that by other two methods.

The experimental procedure of the new method is exact the same as that of the previous methods, i.e., one only needs to measure the necessary FRFs of the two substructures and the whole structure. The feasibility of the experimental procedure has been verified not only in the previous works [15,16], the same experimental procedure has also been used successfully to

Table 7
Identified results of case 5

Parameters	Exact value	Identified value by Eq. (A.11) (error%)	Identified value by Eq. (A.12) (error%)	Identified value by Eq. (21) (error%)
k_1 (N/m)	10,000,000	18224369 (82.24%)	8075138 (19.24%)	10473291 (4.73%)
k_2 (N/m)	200,000	12290163 (6045.08%)	308887 (54.44%)	184337 (7.83%)
k_3 (N/m)	50,000,000	96758735 (93.51%)	67349871 (34.69%)	48753197 (2.49%)
d_1 (N s/m)	1000	6150 (515.00%)	1303 (30.30%)	953 (4.70%)
d_2 (N s/m)	200	2459 (1129.50%)	362 (81.00%)	217 (8.50%)
d_3 (N s/m)	1500	7828 (421.86%)	2135 (42.33%)	1428 (4.80%)

identify different joint parameters [20,21]. Although only simulation results are discussed in this work, it is believed that the conclusion from the experimental results must be same as that from the simulation results.

4. Conclusions

The properties of mechanical joints are very difficult to know by theoretical methods, and generally should be identified by experiments. A new method is proposed in this work to identify the joint parameters directly from the FRFs of the substructures and the whole structure. The problem of the measurement noise with non-Gaussian distribution in the FRFs, and the problem of joints with very different orders of magnitude are especially discussed in this work. The new method uses an error function to select different sets of best data to identify different joints so that the new method can function well under different conditions. The simulation results demonstrate that the proposed new method can always identify the joint parameters with reasonable accuracy even when the results identified by other two existing methods are completely faulty under some strict conditions. The main limitation of the new method is that the joint parameters should be linear. Further efforts could be aimed at applying the method to identify the parameters of joint with a more general model, such as Ref. [22].

Acknowledgements

This work was partially supported by the National Science Council, Taiwan (Contract No. NSC89-2212-E-007-084). This support is hereby gratefully acknowledged.

Appendix A

To show clearly the difference between the method proposed in this work and the previous works [15,16], the mathematical formulations of the previous works are given briefly here.

The first step to minimize the inverse operations is to make difference between Eqs. (6b) and (6c), i.e.,

$$\begin{aligned}[H_{ba}]-[H_{aa}] &= [H_{bb}]_2[H_B]^{-1}[H_{aa}]_1-[H_{aa}]_1+[H_{aa}]_1[H_B]^{-1}[H_{aa}]_1\\ &= -[H_j][H_B]^{-1}[H_{aa}]_1\end{aligned} \tag{A.1}$$

or

$$-[H_B]^{-1}[H_{aa}]_1=[H_j]^{-1}([H_{ba}]-[H_{aa}])=[P_j]([H_{ba}]-H_{aa}]) \tag{A.2}$$

Multiplying Eq. (A.2) by $([H_{aa}]_1+[H_{bb}]_2)$ results in

$$-([H_{aa}]_1+[H_{bb}]_2)[H_B]^{-1}[H_{aa}]_1=([H_{aa}]_1+[H_{bb}]_2)[P_j]([H_{ba}]-[H_{aa}]). \tag{A.3}$$

From Eq. (7), since $[H_{aa}]_1+[H_{bb}]_2=[H_B]-[H_j]$, Eq. (A.3) can be written as

$$-[H_{aa}]_1+[H_j][H_B]^{-1}[H_{aa}]_1=([H_{aa}]_1+[H_{bb}]_2)[P_j]([H_{ba}]-[H_{aa}]). \tag{A.4}$$

Substituting Eq. (A.1) into the left hand side of Eq. (A.4) gives

$$-([H_{aa}]_1+[H_{ba}]-[H_{aa}])=([H_{aa}]_1+[H_{bb}]_2)[P_j]([H_{ba}]-[H_{aa}]). \tag{A.5}$$

The second step to minimize the matrix inverse operation is to expand Eq. (A.5) as

$$\begin{bmatrix} u_{11}, & u_{12}, & \cdots & \cdots & u_{1n}\\ u_{21}, & u_{22}, & \cdots & \cdots & u_{2n}\\ \vdots & & & & \\ \vdots & & & & \\ u_{n1}, & u_{n2}, & \cdots & \cdots & u_{nn}\end{bmatrix} = \begin{bmatrix} \sum s_{1i}t_{i1}p_i, & \sum s_{1i}t_{i2}p_i, & \cdots & \cdots & \sum s_{1i}t_{in}p_i\\ \sum s_{2i}t_{i1}p_i, & \sum s_{2i}t_{i2}p_i, & \cdots & \cdots & \sum s_{2i}t_{in}p_i\\ \vdots & & & & \\ \vdots & & & & \\ \sum s_{ni}t_{i1}p_i, & \sum s_{ni}t_{i2}p_i, & \cdots & \cdots & \sum s_{ni}t_{in}p_i\end{bmatrix} \quad \text{for } i=1,2,\ldots,n, \tag{A.6}$$

where $p_i=k_i+\mathrm{j}\omega d_i$, and n is the number of the joints in Fig. 1. Noting that $[P_j]$ is a diagonal matrix, as shown in Eq. (4). From Eq. (A.6), the diagonal terms were suggested in Ref. [15] to extract the parameters p_i, i.e.,

$$\begin{Bmatrix} u_{11}\\ u_{22}\\ \vdots\\ \vdots\\ u_{nn}\end{Bmatrix} \equiv \begin{Bmatrix} U\end{Bmatrix}_{n\times 1} \begin{bmatrix} s_{11}t_{11}, & s_{12}t_{21}, & \cdots & \cdots & s_{1n}t_{n1}\\ s_{21}t_{12}, & s_{22}t_{22}, & \cdots & \cdots & s_{2n}t_{n2}\\ \vdots & & & & \\ \vdots & & & & \\ s_{n1}t_{1n}, & s_{n2}t_{2n}, & \cdots & \cdots & s_{nn}t_{nn}\end{bmatrix}_{n\times n} \begin{Bmatrix} p_1\\ p_2\\ \vdots\\ \vdots\\ p_n\end{Bmatrix}_{n\times 1} \tag{A.7}$$

or in a compact form as

$$\{U\}_{n\times 1}\equiv[Q]_{n\times n}\{\bar{P}\}_{n\times 1}. \tag{A.8}$$

One can find in Eq. (A.8) that the joint parameters $\{\bar{P}\}$ can be found only with one inverse operation on the $[Q]$ matrix. The difference between Eqs. (8) and (A.8) is very significant. Noting

that the vector $\{U\}$ and the matrix $[Q]$ are function of frequency and contain the information of the FRFs of the whole structure and the substructures. If the joint parameters are constant (frequency independent), then theoretically the FRFs only at one frequency should be used to extract the joint parameters. However, in order to smooth the random noise, the FRFs at many frequencies should be used in practice. For instance, if the FRFs are known at some discrete frequencies, $\omega_1, \omega_2, \ldots, \omega_m$, then for each frequency one has a set of n simultaneous equation like Eq. (A.8), the total equation can be written as

$$\begin{Bmatrix} \{U(\omega_1)\}_{n\times 1} \\ \{U(\omega_2)\}_{n\times 1} \\ \vdots \\ \{U(\omega_m)\}_{n\times 1} \end{Bmatrix}_{mn\times 1} = \begin{bmatrix} [Q(\omega_1)]_{n\times n} \\ [Q(\omega_2)]_{n\times n} \\ \vdots \\ [Q(\omega_m)]_{n\times n} \end{bmatrix} \begin{Bmatrix} \bar{P} \end{Bmatrix}_{n\times 1} \tag{A.9}$$

or in a compact form

$$\{\bar{U}\}_{mn\times 1} = [\bar{Q}]_{mn\times n}\{\bar{P}\}_{n\times 1}. \tag{A.10}$$

The least-squares method can then be used to obtain the joint parameter as

$$\{\bar{P}\}_{n\times 1} = ([\bar{Q}]^{\mathrm{H}} \cdot [\bar{Q}])^{-1}[\bar{Q}]^{\mathrm{H}}\{\bar{U}\}_{mn\times 1}, \tag{A.11}$$

where $[\bar{Q}]^{\mathrm{H}}$ represents the conjugate transposed matrix of $[\bar{Q}]$.

Eq. (A.11) is the identification equation proposed in Ref. [15], and will be used to compare with the new method proposed in this work. If the FRFs are measured with an FFT analyzer, then generally there are 400 or 800 discrete frequencies in each FRF spectrum. The method [15] used all the data of the FRFs at 400 or 800 discrete frequencies to identify the parameter without any selection. On the contrary, the method proposed in Ref. [16] used the condition number of the $[Q]$ matrix in Eq. (A.8) to select the "well-conditioned" data for identification. If the FRFs are measured at some discrete frequencies, $\omega_1, \omega_2, \ldots, \omega_m$, then one can find the condition number of $[Q]$ matrix for each frequency. If the average value of the condition number found at the m frequencies is denoted by C_m, then the $[Q]$ matrix with condition number lower than C_m is defined as "well-conditioned" data [16], and used to identify the joint parameters from Eq. (A.8) by direct matrix inverse in each frequency. In other words, if m is the number of the discrete frequencies, the number of frequencies used for identification is $m/2$. The average values of the identified parameters from the $m/2$ frequencies are defined as the final identified values. In order to compare the method [16] with the new method proposed in this work, the equation used in Ref. [16] is given here as

$$\{\bar{P}_{ave}\}_{n\times 1} = \frac{1}{N}\left(\sum_{j=1}^{N} ([Q(\omega_j)]^{-1}\{U(\omega_j)\})\right), \tag{A.12}$$

where ω_j indicates the frequencies selected by the method [16], and N is the total number of frequencies used for identification.

Appendix B

In this appendix, the structure and noise distribution of case 2 in the main text is used as an example to show the statistical relationship between $R_e(E_i)$ (or $I_m(E_i)$) and $|R_e(\delta_{ii})|$ (or $|I_m(\delta_{ii})|$). The selection criteria of the number of frequencies used for identification are also discussed in this appendix.

As mentioned, there are 400 discrete frequencies in each FRF spectrum. For simplicity, we discuss only the relationship between $R_e(E_i)$ and $|R_e(\delta_{ii})|$. For each frequency ω_k, one can obtain a set of data $(R_e(E_i(\omega_k)), |R_e(\delta_{ii}(\omega_k))|)$ from the result of Eq. (14). Noting that in practical experiment one can only know the $R_e(E_i(\omega_k))$ and cannot know the $R_e(\delta_{ii}(\omega_k))$. However, in the simulation one can know the $R_e(\delta_{ii}(\omega_k))$ because one knows the exact values of the joint parameters. If a x–y rectangular co-ordinate is used, and the horizontal x-axis represents the value of $R_e(E_i)$ and the vertical y-axis represents the value of $R_e(\delta_{ii})$, then each data set $(R_e(E_i(\omega_k)), |R_e(\delta_{ii}(\omega_k))|)$ is a data point in the x–y plane. Therefore, from 400 frequencies there are 400 points in the x–y plane, as shown in Fig. 6 for $i = 1$. Noting that in this simulation case, $i = 1, 2, 3$. For $i = 2$, and 3, one can find the same characteristics like Fig. 6. To show the statistical relationship between $R_e(E_i)$ and $|R_e(\delta_{ii})|$, $R_e(E_i)$ and $|R_e(\delta_{ii})|$ are considered as two random variables, indicated as a, and b. The correlation coefficient of two random variables is defined as [23]

$$\rho_{ab} = \frac{E[(a - m_a)(b - m_b)]}{\sigma_a \sigma_b},$$

where σ_a and σ_b represent the standard deviations of a and b, respectively; m_a and m_b represent the mean values of a and b, respectively; $E[(a - m_a)(b - m_b)]$ represents the expect value (mean value)

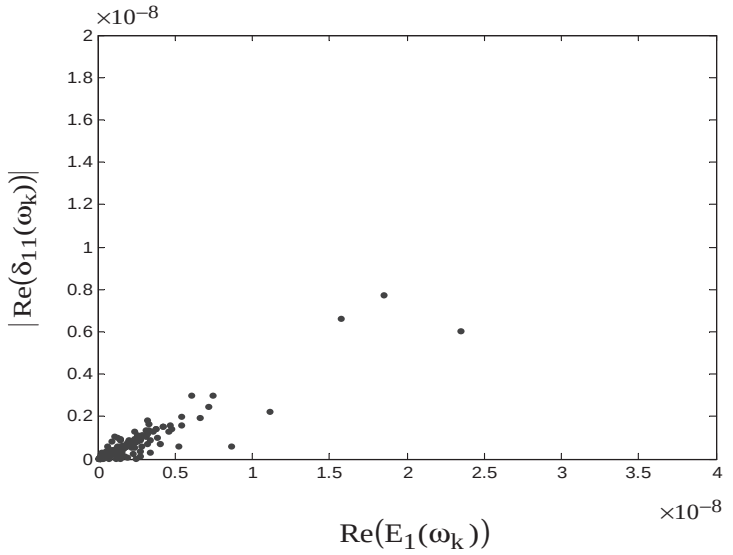

Fig. 6. The statistical relationship between $R_e(E_1(\omega_k))$ and $|R_e(\delta_{11}(\omega_k))|$, $k = 1, 2, \ldots, 400$.

of $[(a-m_a)(b-m_b)]$. One knows that $0 \leqslant |\rho_{ab}| \leqslant 1$. The correlation coefficient of the two random variables in Fig. 6 is 0.9868. In other words, $R_e(E_1(\omega_k))$ and $|R_e(\delta_{11}(\omega_k))|$ are statistically highly correlated. That means if one chooses a frequency with which the $R_e(E_1)$ is very small (among other frequencies), then the possibility of $|R_e(\delta_{11})|$ with very small value is very high. The $|R_e(\delta_{11})|$ represents the error (absolute value) of the identified k_1. Therefore, one can choose some frequencies with which the $R_e(E_1)$ has relative small value (among the 400 frequencies) to identify k_1, and the average value from these frequencies is defined as the identified value of k_1, as defined in Eq. (21).

The relationship between the $I_m(E_1)$ and $|I_m(\delta_{11})|$ is the same as that discussed above. Therefore, one can use the $I_m(E_1)$ as an indicator to select the frequencies to identify d_1. That is why the proposed new method uses the $R_e(E_i)$ as an indicator to select frequencies to identify k_i, and uses $I_m(E_i)$ as an indicator to select frequencies to identify d_i. It should be emphasized that the new method uses data at different frequencies to identify different parameters. This is the very important feature of the new method. That is why the proposed new method can adapt itself to handle different conditions. As to the question how many frequencies of FRFs should be used to identify each parameter, 10% of the measured frequencies and at least 40 frequencies are recommended in this work. That means the number of discrete frequencies at each FRF spectrum should not be less than 400 in order to select the best 10% (40 frequencies) data for identification. Of course, this recommendation is not very strict, some more or less data are acceptable. The basic rules are :(1) the number of the measured frequencies of the FRFs should be large enough in order to have enough data base to select the best data for identification, (2) the number of the selected frequencies should be kept to a minimum value (i.e., only the best data are selected), but should be large enough to show the statistical linear relationship between $R_e(E_i)$ and $|R_e(\delta_{ii})|$. Based on these

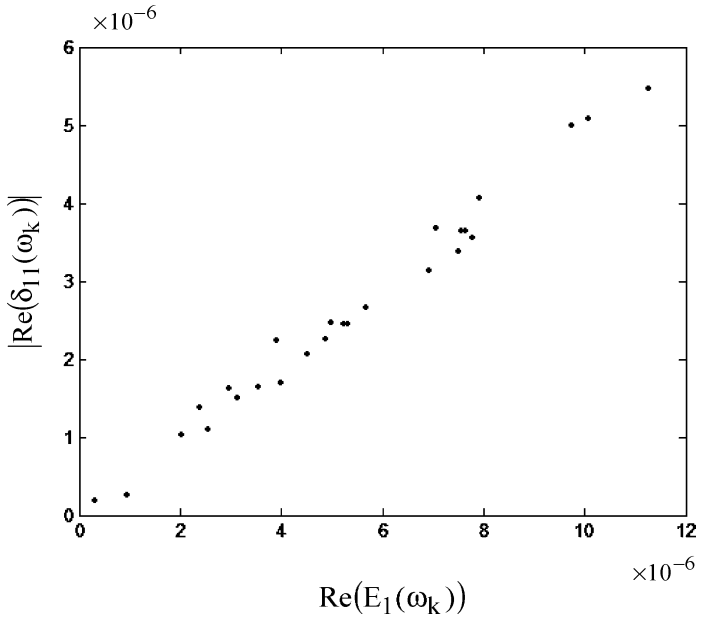

Fig. 7. The statistical relationship between the forty smallest values of $R_e(E_1(\omega_k))$ and the corresponding $|R_e(\delta_{11}(\omega_k))|$.

basic rules, different types of structure and noise distribution have been investigated, and the final recommended values are: the number of the measured frequencies should be larger than 400, and the number of the selected frequencies should be about 10% of total measured frequencies. If the FRFs are measured with standard spectrum analyzer, generally there are 400 or 800 discrete frequencies in each spectrum. Then, 40 or 80 frequencies should be used for the identification of each joint parameter. Fig. 7 shows the relationship between the smallest 40 data of $R_e(E_1)$ and the corresponding $|R_e(\delta_{11})|$ of Fig. 6. The correlation coefficient between the $R_e(E_1)$ and $|R_e(\delta_{11})|$ is 0.966. It indicates that 40 frequencies is enough to guaranty a statistical linear relationship between $R_e(E_1)$ and $|R_e(\delta_{11})|$.

References

[1] A.R. Thoren, Derivation of mass and stiffness from dynamic test data, Paper Number 72-346, American Institute of Aeronautics and Astronautics, 1972.

[2] L. Eckert, H. Freund, W. Schilling, Identification von Strukturmatrizen aus dynamischen Nachgiebigkeiten, *VDI Bericht* 536 (1984) 255–272.

[3] C.-P. Fritzen, Identification of mass, damping and stiffness matrices of mechanical systems, *American Society of Mechanical Engineers Journal of Vibrations, Acoustics, Stress and Reliability in Design* 108 (1986) 9–16.

[4] J.H. Wang, Mechanical parameters identification, with special consideration of noise effects, *Journal of Sound and Vibration* 125 (1988) 151–167.

[5] J.E. Mottershead, M.I. Friswell, Model updating in structural dynamics: a survey, *Journal of Sound and Vibration* 162 (1993) 347–375.

[6] C. Mares, M.I. Friswell, J.E. Mottershead, Model updating using robust estimation, *Mechanical Systems and Signal Processing* 16 (2002) 169–183.

[7] H.G. Natke, Updating computational models in frequency domain based on measured data: a survey, *Probabilistic Engineering Mechanics* 3 (1998) 28–35.

[8] J. Wang, P. Sas, A method for identifying parameters of mechanical joints, *American Society of Mechanical Engineers Journal of Applied Mechanics* 57 (1990) 337–342.

[9] J.X. Yuan, X.M. Wu, Identification of the joint structural parameters of machine tool by DDS and FEM, *American Society of Mechanical Engineers Journal of Engineering for Industries* 107 (1985) 64–69.

[10] R. Ren, C.F. Beards, Identification of "effective" linear joints using coupling and joint identification techniques, *American Society of Mechanical Engineers Journal of Vibration and Acoustics* 121 (1998) 331–338.

[11] A.S. Nobari, D.A. Robb, D.J. Ewins, A new modal-based method for structural dynamic model updating and joint identification, *Proceedings of the 10th International Modal Analysis Conference*, Vol. 1, San Diego, CA, 1992, pp. 741–750.

[12] J.E. Mottershead, M.I. Friswell, G.H.T. Ng, J.A. Brandon, Geometric parameters for finite element model updating of joints and constraints, *Mechanical Systems and Signal Processing* 10 (1996) 171–182.

[13] W.L. Li, A new method for structural model updating and joint stiffness identification, *Mechanical Systems and Signal Processing* 16 (2002) 155–167.

[14] J.S. Tsai, Y.F. Chou, The identification of dynamic characteristics of a single bolt joint, *Journal of Sound and Vibration* 125 (1988) 487–502.

[15] J.H. Wang, C.M. Liou, Identification of parameters of structural joints by use of noise-contaminated FRFs, *Journal of Sound and Vibration* 142 (1990) 261–277.

[16] J.H. Wang, C.S. Liou, The use of condition number of a FRF matrix in mechanical parameter identification, *American Society of Mechanical Engineers Conference, Vibrations of Mechanical Systems and the History of Mechanical Design*, DE-Vol. 63, NM, 1993, pp. 117–124.

[17] H.Y. Hwang, Identification techniques of structure connection parameters using frequency response functions, *Journal of Sound and Vibration* 212 (1998) 469–479.

[18] J.H. Wang, S.B. Horng, Investigation of the tool-holder system with a taper Angle 7:24, *International Journal of Machine Tools and Manufacture* 34 (1994) 1163–1176.
[19] J.H. Wang, M.H. Lee, Identification of bearing parameters of grinder's spindle, *12th National Conference on Mechanical Engineering*, Chia-Yi, Taiwan, 1995, pp. 391–400.
[20] P. Lancaster, M. Tismenetsky, *The Theory of Matrix*, 2nd Edition, Academic Press, New York, 1985.
[21] M.J. Ratcliffe, N.A.J. Lieven, An investigation into the effects of frequency response function estimators on model updating, *Mechanical Systems and Signal Processing* 13 (2) (1999) 315–334.
[22] M.J. Ratcliffe, N.A.J. Lieven, A generic element-based method for joint identification, *Mechanical System and Signal Processing* 14 (1) (2000) 3–28.
[23] D.E. Newland, *Random Vibration, Spectral and Wavelet Analysis*, 3rd Edition, Longman Scientific & Technical, New York, 1993.